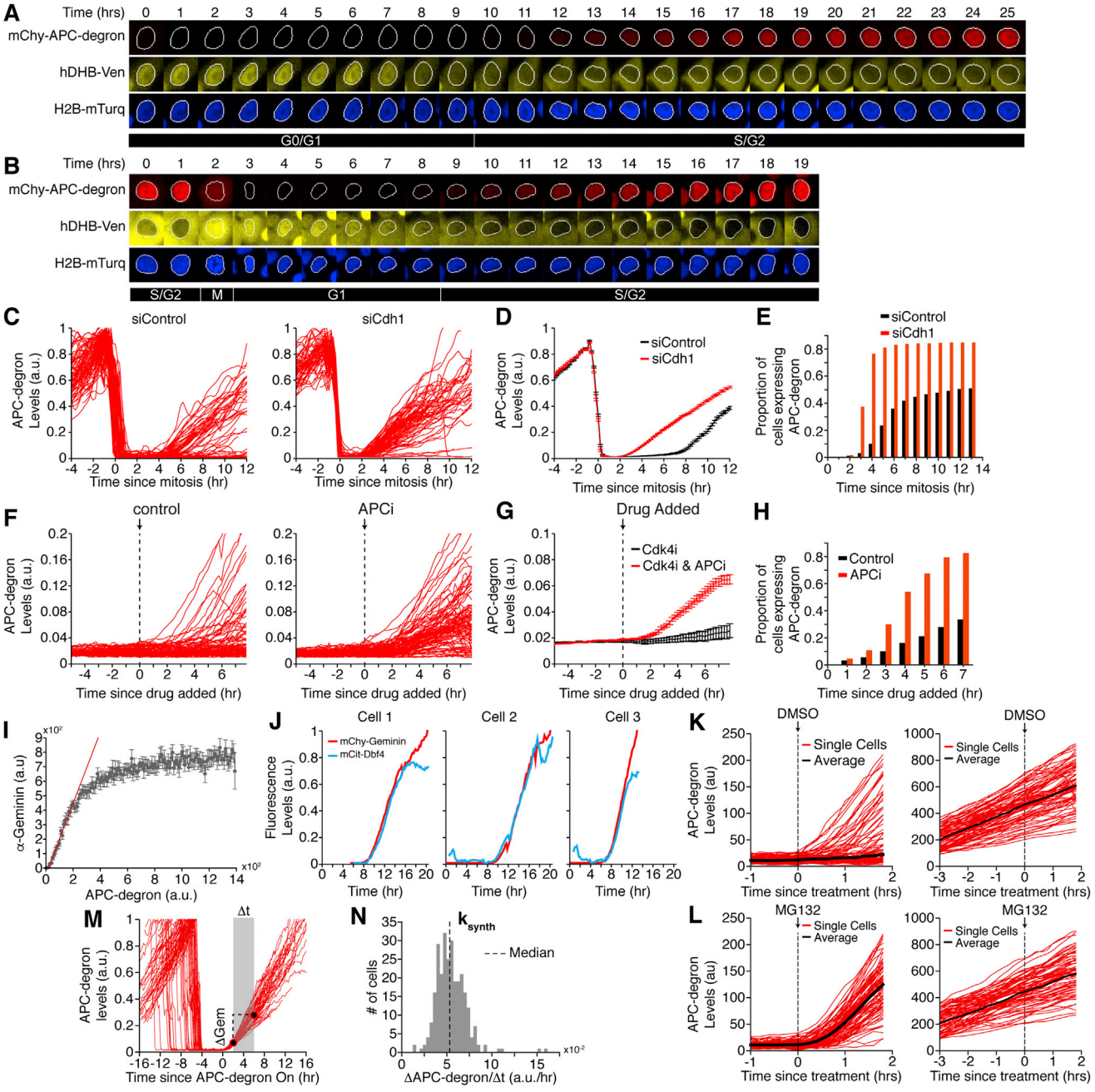


**Figure S1. APC Activity Derived from Concentration Changes of the APC-Degron Reporter, Related to Figure 1**

(A and B) Image montage of a single-cell expressing APC-degron, hDHB-mVenus (Cdk2 sensor), and H2B-mTurquiose (used to both track and mask nuclei). Images are from the same cell as in Figures 1C and 1D respectively. Images were taken every 12min, but only 1 hr time intervals are shown due to space constraints. All images 33 μm × 33 μm.

(C) Single-cell traces of APC-degron treated with either Control siRNA or Cdh1 siRNA. Traces are alligned to the time of mitosis (n = 108, control; n = 95, siCdh1).

(D) Median trace ± SEM from (C).

(E) Proportion of cells from (C) as a function of time since mitosis. Cdh1 knockdown causes an early rise in APC-degron levels.

(F) Single-cell traces of APC-degron levels in HeLa cells treated with either DMSO or the small molecule inhibitor proTAME (10mM). Traces are alligned to the time of mitosis (n = 88, control; n = 95, APCi).

(G) Median trace ± SEM from (F).

(H) Proportion of cells from (F) as a function of time since mitosis. Treatment with the APC inhibitor causes an early rise in APC-degron levels.

*(legend continued on next page)*

(I) MCF-10A Cells expressing APC-degron were fixed and stained for α-Geminin. Cells were binned by APC-degron levels and data represent median value of each bin ± SEM (n = 12 wells; ~5,000 cells/well). APC-degron levels are linearly correlated to endogenous Geminin at low levels (Red line), but the antibody staining of endogenous Geminin saturates at higher levels.

(J) Representative examples of single HeLa cells transiently transfected with the APC-degron reporter and mCitrine-Dbf4, both under the control of constitutive promoters. (representative examples out of 5000 cells analyzed).

(K and L) Single-cell traces of APC-degron treated with or without 10 μM MG132 at the indicated time. Left panel: Only cells with low APC-degron levels at the time of drug addition were considered. Cells with high APC-degron levels in DMSO treated condition are cells that happened to enter S phase. Right panel: only cells with high APC-degron levels, and therefore $APC^{Cdh1}$ activity was off, at the time of drug addition were considered. (K) DMSO and (L) 10 μM MG132.

(M) Cells expressing APC-degron were aligned in silico to the time when APC-degron first starts to accumulate. The promoter region of APC-degron is unregulated and thus the rate of accumulation was linear. To estimate the rate of APC-degron accumulation, or ksynth, the change in APC-degron levels was calculated over a 4 hr time window 2-6 hr after APC-degron first starts to accumulate.

(N) Histogram of the ksynth from single-cells. The median ksynth was used to convert APC-degron measurements into APC activity.

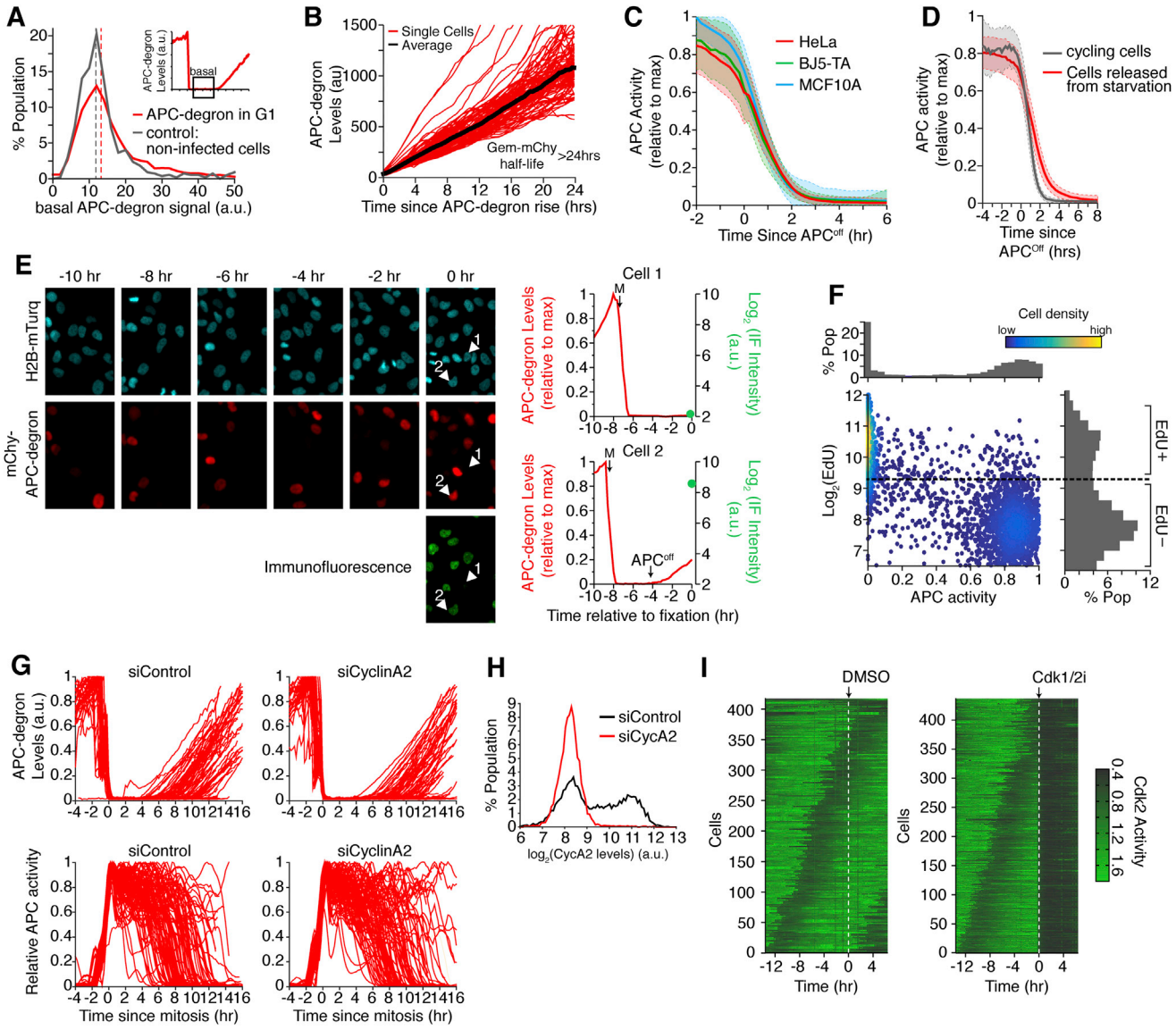


**Figure S2. Cyclin E/Cdk2 and Not CyclinA/Cdk2 Plays a Role in APC$^{Cdh1}$ Inactivation at the G1/S Transition, Related to Figure 2**

(A) Histogram of basal APC-degron levels. Grey line is from un-infected control cells. Red line is from G1 cells expressing APC-degron (see inset). Dashed line is population mean.

(B) Single-cell traces of APC-degron levels. Only cells that accumulated APC-degron for 24 hr are shown. Indicates half-life of APC-degron when APC$^{Cdh1}$ is inactivated is greater than 24 hr.

(C) Median ± SD APC activity traces aligned to the time of APC$^{Cdh1}$ inactivation for multiple cell lines. n = 277, BJ5TA; n = 261, HeLa; n = 1429, MCF10A.

(D) Median ± SD APC activity traces for cells released from 48 hr of mitogen starvation (Right) and cycling cells (Left). Traces are aligned to the time APC$^{Cdh1}$ turns off. n = 133, mitogen starved; n = 71, cycling cells.

(E) Live-cell imaging of fluorescent sensors followed by fixing and staining for specific proteins. This technique allows us to obtain, for each cell, the specific point in the cell cycle, APC activity, and levels of the stained protein. Left: Time-lapse images. Arrows show 2 cells in each fluorescent channel. Right: Single-cell traces and immunofluorescence (IF) intensity for the same two cells. Scale bar is 10 μm.

(F) Density scatterplot of APC activity and levels of EdU incorporation in single cells from live-cell imaging followed by fixed-cell staining. Single-parameter histograms are shown above and to the right.

(G) Single HeLa cell traces of APC-degron levels (top) or APC activity (bottom) treated with either control siRNA or cyclin A2 siRNA.

(H) Cells from (G) were immunostained with anti-cyclin A after live-cell imaging to confirm efficient knockdown of cyclin A2. Data are a histogram of cyclin A2 levels in single cells.

(I) Heatmap of Cdk2 activity. Data show that the Cdk1/2 inhibitor used in Figures 2I and 2J is sufficient to inhibit Cdk2 activity.

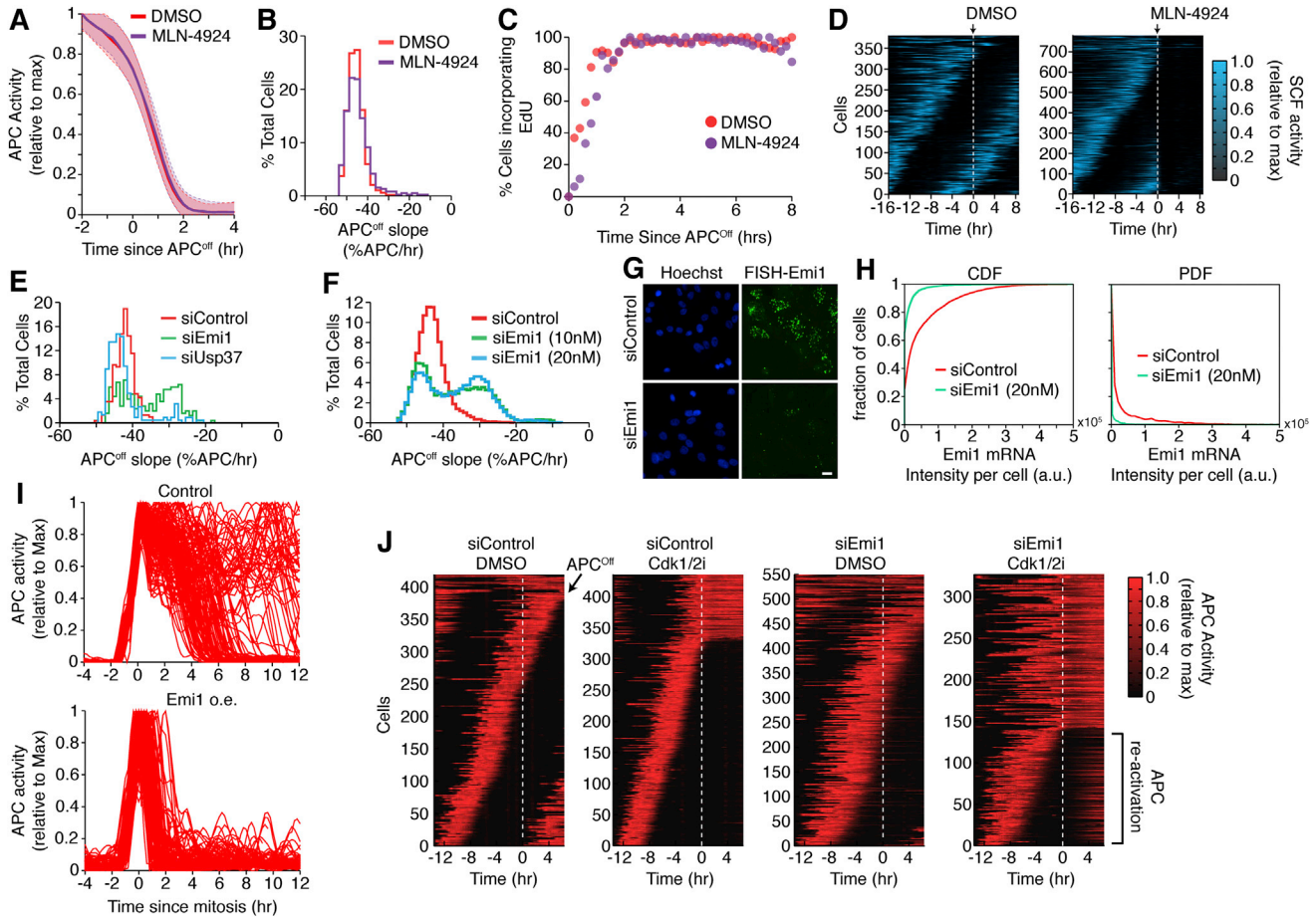


**Figure S3. Emi1 Makes APC$^{Cdh1}$ Inactivation Rapid and Irreversible, Related to Figure 3**

(A) Median ± SD APC activity traces aligned to the time of APC$^{Cdh1}$ inactivation for cells treated with either DMSO or the neddylation inhibitor MLN-4954. n = 128, DMSO; n = 387, MLN-4924.

(B) Histogram of the APC inactivation slope from (A).

(C) Cells were pre-imaged to determine the time since APC inactivation and then fixed and stained for EdU incorporation. Cells were binned by the time since APC inactivation and data are the percent cells that are EdU positive in each bin.

(D) Heatmap of SCF activity. Cells were stably infected with the FUCCI sensor Cdt1-mVenus. We used the same equation as for APC activity to convert Cdt1-mVenus levels into SCF activity. Cells were sorted by the time of mitosis and each line in the heatmap is a single cell. Cells were treated with either DMSO or MLN-4924 at the indicated time. Data show that MLN-4924 rapidly inactivates SCF activity.

(E) Histogram of APC inactivation rates in cells treated with Emi1 or Usp37 siRNA.

(F) Histogram of APC inactivation rates in cells treated with the indicated concentrations of Emi1 siRNA.

(G) Single-molecule mRNA FISH of Emi1 on cells treated with or without Emi1 siRNA. Cells were fixed 18 hr post-transfection with siRNA. Scale bar is 10 μm.

(H) Histogram (Right: Cumulative distribution function, CDF; Left: Probability density function, PDF) of single-cell Emi1 mRNA levels as measured in (G). Total fluorescent intensity per cell. Lack of two clear peaks means data are not bimodal.

(I) Single-cell APC activity traces aligned to mitosis. Cells were expressing either empty vector or mCitrine-Emi1.

(J) Heatmap of single-cell APC activity traces from Figures 3G–3I. Cells were treated with either control or Emi1 siRNA at the beginning of the imaging period. Either DMSO or Cdk1/2 inhibitor was added at time 0, indicated by the white dashed line. Cells that reactivated the APC$^{Cdh1}$ post-drug treatment are indicated.

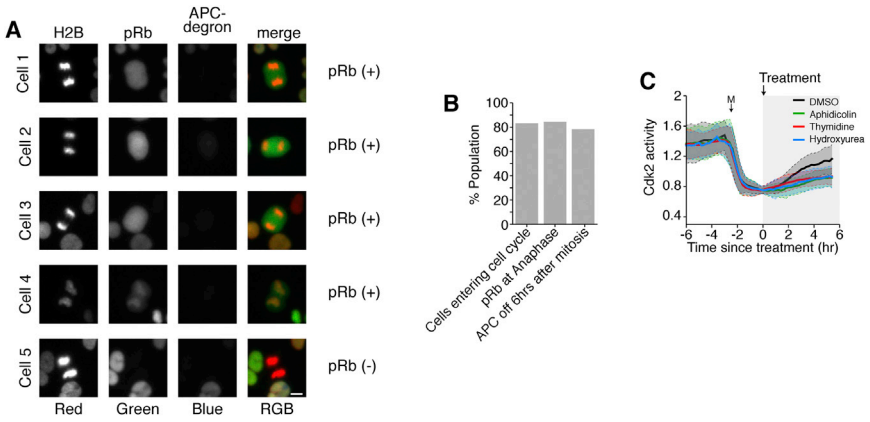


**Figure S4. Rb Is Already Hyper-Phosphorylated During the Anaphase in Cycling Cells, Related to Figure 4**

(A) MCF-10A cell stably expressing H2B-mTurquiose and APC-degron. Cells were fixed and stained for pRb807/811. Shown are 5 representative cells in anaphase (APC-degron is degraded). Scale bar is 10 μm.

(B) Bar graph comparing the percentage of cells entering the cell cycle right after mitosis (N > 5000), the percentage of cells with phosphorylated Rb (807/811) at anaphase (n = 86), and the percentage of cells with inactivated $APC^{Cdh1}$ within 6 hr of mitosis (n = 567).

(C) Median traces ± SD of Cdk2 activity in cells treated with the indicated drug. Only cells in G1 phase at the time of drug addition were considered. "M" denotes time of mitosis. See Figure 4L for the corresponding APC activity traces.

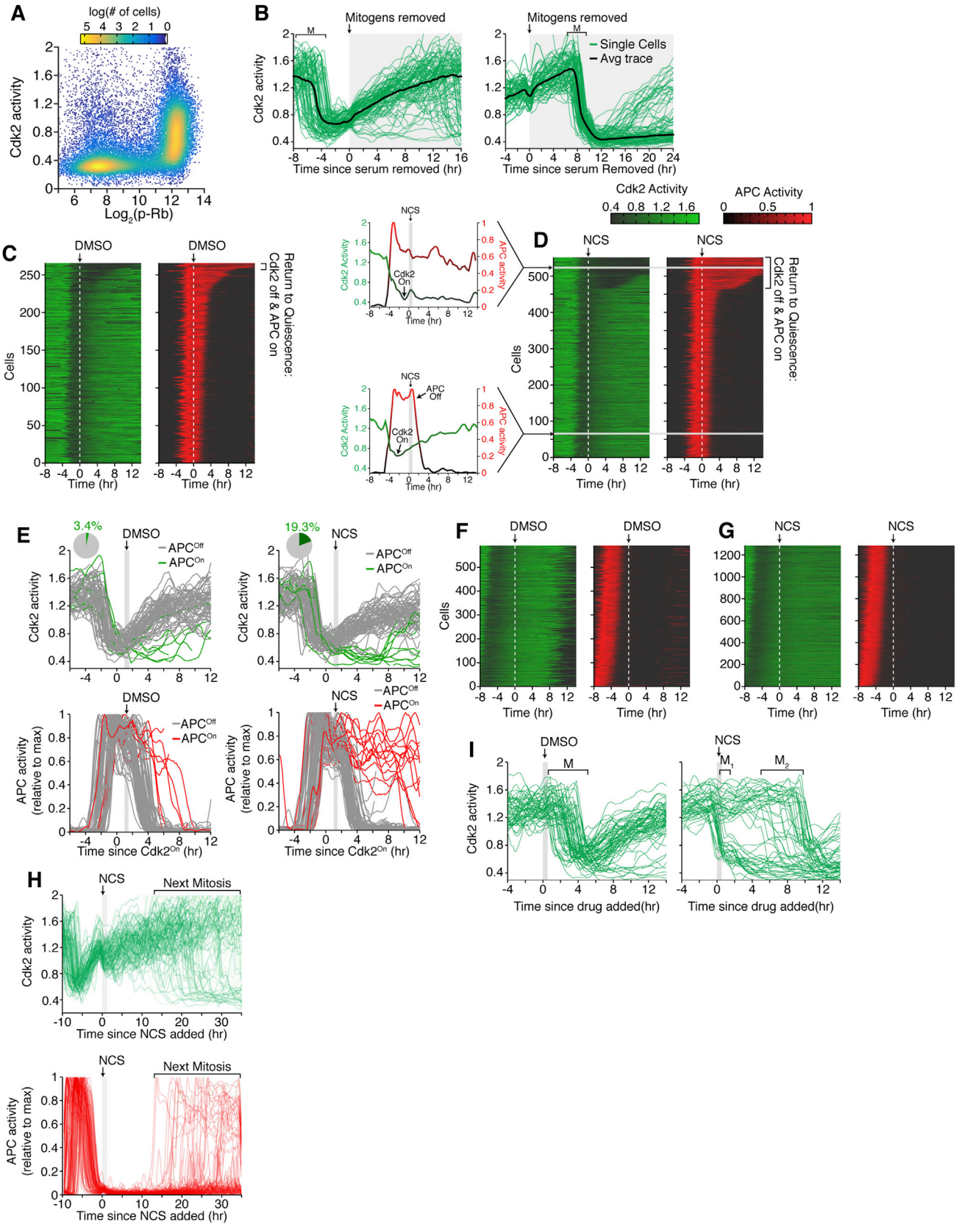


*(legend on next page)*

**Figure S5. Stress Causes Reversible Cell-Cycle Exit after the Restriction Point but before APC$^{Cdh1}$ Inactivation, Related to Figure 5**

(A) Density scatterplot of pRb807/811 versus Cdk2 activity in single cells. Cdk2 activity rises after Rb becomes hyper-phosphorylated, indicating cells with high Cdk2 activity have passed the Restriction Point.

(B) Mitogens were removed from asynchronous cells. Left panel: Mitogens removed after the initial rise in Cdk2 activity. Almost all cells continued to increase Cdk2 activity despite the absence of mitogens, indicating they have passed the restriction point. Right panel: mitogens removed before Mitosis. Almost all cells have low Cdk2 activity after mitosis, indicating they are in a G0-like state. Black line is median Cdk2 activity. Arrow indicates when mitogens were removed. Gray band represents time when mitogens were absent. M, mitosis.

(C and D) Heatmap of Cdk2 and APC activity in cells exposed to stress after Cdk2 activity started to rise. Two individual cells treated with NCS are highlighted, showing how single-cell activity data are encoded in the heatmap. Cells are sorted by the time APC inactivated relative to drug addition. Brackets indicate the population of cells that inactivated Cdk2 and never inactivated APC despite crossing the Restriction Point. Compare to control in (C). (C) DMSO, (D) 40ng/mL Neocarzinostatin.

(E) Single-cell traces of Cdk2 and APC activity in cells exposed to the indicated conditions. Cells were used to obtain median traces in Figures 5C and 5D and the heatmaps in Figures S5C and S5D. Pie Chart indicates the percentage of cells inactivating Cdk2 and maintaining APC activity (colored) or continuing into the cell cycle and inactivating the APC (dark gray). Light gray bar indicates the time cells were exposed to the indicated conditions.

(F and G) Heatmap of Cdk2 and APC activity in cells exposed to stress after APC$^{Cdh1}$ inactivation. Cells are sorted by the time APC inactivated relative to drug addition. (F) DMSO, (G) 40ng/mL Neocarzinostatin (NCS).

(H) Single-cell traces of Cdk2 activity (top) and APC activity (bottom) in cells exposed to NCS after APC$^{Cdh1}$ inactivation. Period of NCS exposure shown in gray band. Cells that entered mitosis after NCS treatment are indicated. Note the second mitosis is marked by rapidly falling Cdk2 activity and rapidly increasing APC activity.

(I) Single-cell traces of Cdk2 activity in cells exposed to DMSO or NCS. Only cells exposed to stress just prior to Mitosis are considered. NCS treatment led to a delay in the onset of Mitosis (M) compared to DMSO treated cells.

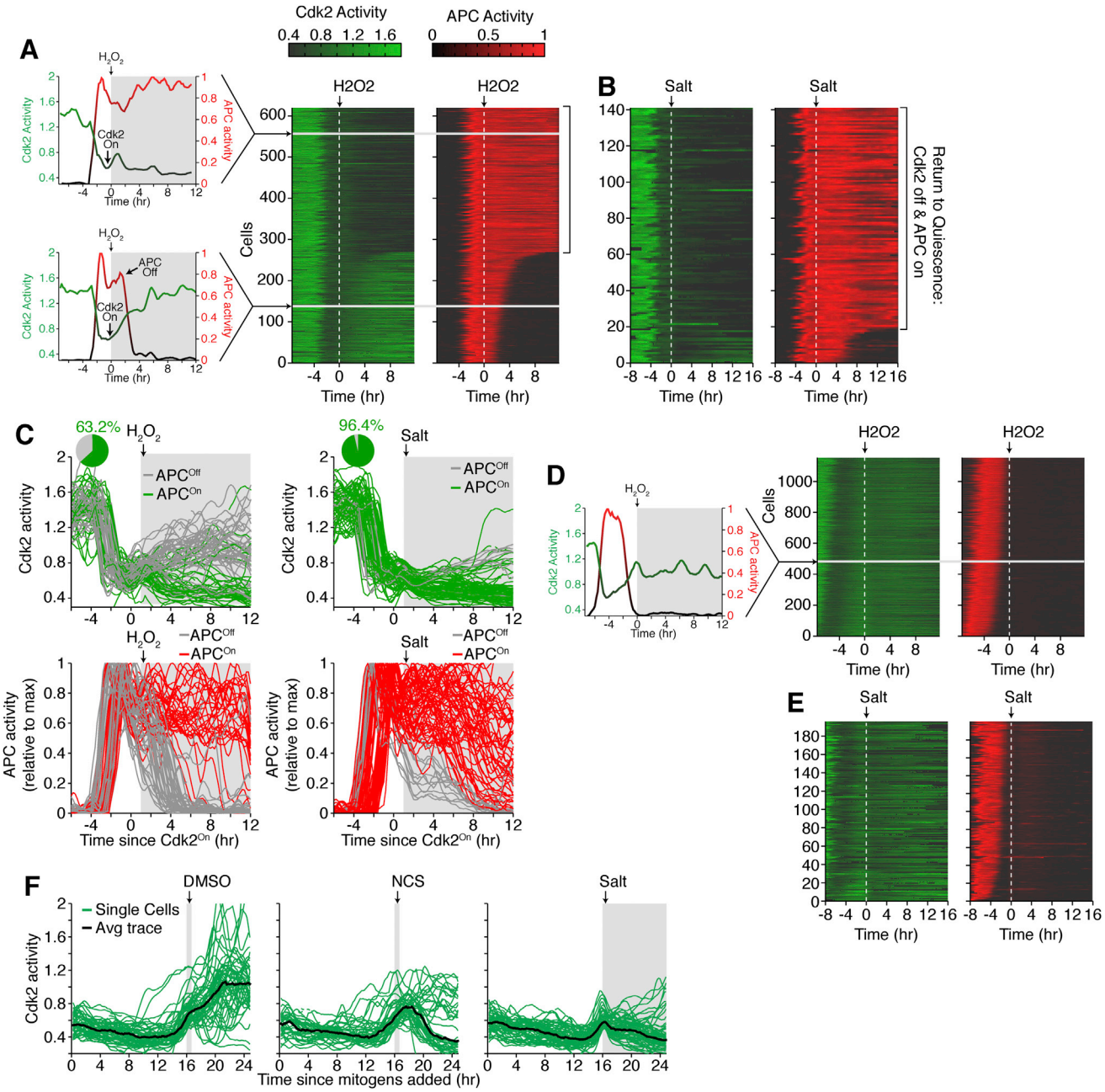


**Figure S6. Other Stresses also Cause Reversible Cell Exit after the Restriction Point but Before APC$^{Cdh1}$ Inactivation, Related to Figure 6**

(A and B) Heatmap of Cdk2 and APC activity in cells exposed to stress after Cdk2 activity started to rise. Two individual cells treated with hydrogen peroxide are highlighted, showing how single-cell activity data are encoded in the heatmap. Cells are sorted by the time APC inactivated relative to drug addition. Brackets indicate the population of cells that inactivated Cdk2 and never inactivated APC despite crossing the restriction point. (A) 200 μM Hydrogen peroxide (H2O2), (B) 100mM NaCl (Salt).

(C) Single-cell traces of Cdk2 and APC activity in cells exposed to the indicated conditions. Cells were used to obtain median traces in Figures 6B and 6C and the heatmaps in Figures S6A and S6B. Pie Chart indicates the percentage of cells inactivating Cdk2 and maintaining APC activity (colored) or continuing into the cell cycle and inactivating the APC (dark gray). Light gray bar indicates the time cells were exposed to the indicated conditions.

(D and E) Heatmap of Cdk2 and APC activity in cells exposed to stress after APC$^{Cdh1}$ inactivation. A single-cell treated with hydrogen peroxide is highlighted, showing how single-cell activity data are encoded in the heatmap. Cells are sorted by the time APC inactivated relative to drug addition. (D) 200 μM Hydrogen peroxide (H2O2), (E) 100mM NaCl (Salt).

(F) Single-cell Cdk2 activity traces in cells released from serum starvation and treated with the indicated stress. Only cells that had begun to activate Cdk2 but had not yet inactivated APC$^{Cdh1}$ were considered.

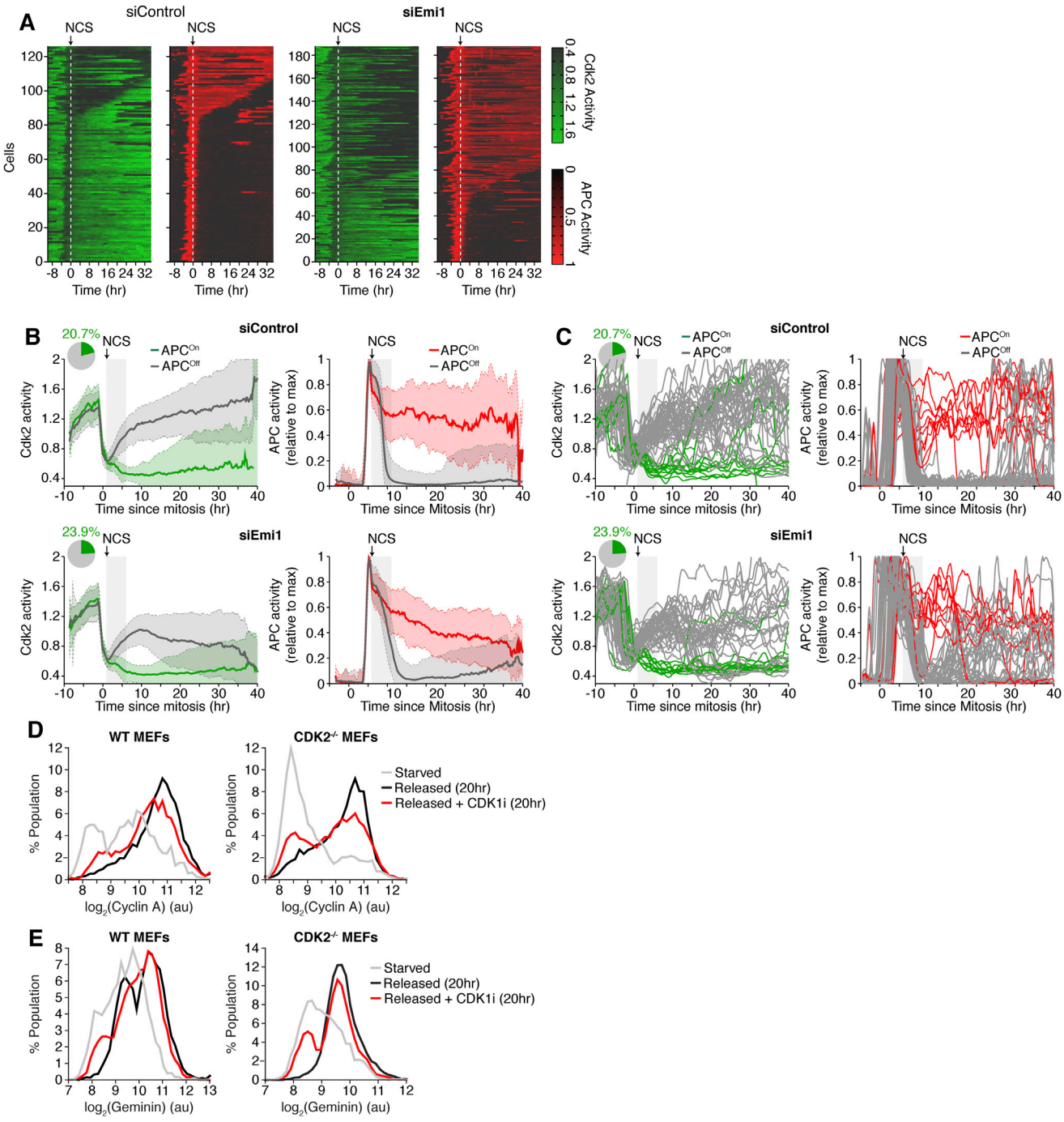


**Figure S7. Emi1 Makes APC$^{Cdh1}$ Inactivation Irreversible when Stress is Encountered, Related to Figure 7**

(A) Heatmap of Cdk2 and APC activity in cells exposed to stress after Cdk2 activity started to rise. Cells are sorted by the time APC inactivated relative to NCS addition. Cells were pre-treated with either contorl siRNA or Emi1 siRNA.

(B) Median traces ± SD of Cdk2 and APC activity in cells exposed to NCS and treated with either control siRNA (Top) or Emi1 siRNA (bottom). Light gray band represents time when cells were exposed to NCS. Traces are colored if Cdk2 inactivated despite initially turning on or gray if Cdk2 stayed active and APC$^{Cdh1}$ inactivated. Inset: Pie chart indicated the percentage of cells that inactivated Cdk2 activity despite initially turning on. n = 328, siControl; n = 506, siEmi1.

(C) Single-cell traces of Cdk2 and APC activity in cells exposed to NCS after Cdk2 activity started to rise (Figure S7B). Cells were treated with either control siRNA or Emi1 siRNA. Gray band represents time when cells were exposed to NCS. Traces are colored dark if Cdk2 inactivated despite initially turning on or colored light if Cdk2 stayed active and APC$^{Cdh1}$ inactivated.

(D and E) Histogram of Cyclin A (D) or Geminin (E) levels as measured by immunofluorescence. Wild-type or Cdk2−/− MEFs were starved for 48 hr and then released with and without the Cdk1 inhibitor RO-3306 (10mM). Cells were fixed and stained 20 hr post-release. n∼5000 cells per condition.

**Cell, Volume *166***

## Supplemental Information

# Irreversible $APC^{Cdh1}$ Inactivation Underlies the Point of No Return for Cell-Cycle Entry

**Steven D. Cappell, Mingyu Chung, Ariel Jaimovich, Sabrina L. Spencer, and Tobias Meyer**

## Supplemental Experimental Procedures

### Cell Culture Media

MCF10A cells were cultured in phenol red-free DMEM/F12 (Invitrogen) supplemented with 5% horse serum, 20,000 pg/mL EGF, 10 μg/mL insulin, 0.5 μg/mL hydrocortisone, 100 ng/mL cholera toxin, 50 U/mL penicillin, and 50 μg/mL streptomycin. For experiments where mitogens were withdrawn, cells were washed three times and then incubated with GM-GFS medium (DMEM/F12 supplemented with 0.3% BSA, 0.5 μg/mL hydrocortisone, 100 ng/mL cholera toxin, 50 U/mL penicillin, and 50 μg/mL streptomycin). Where indicated, cells were treated with 200 μM $H_2O_2$ in full growth medium. HeLa cells were cultured in DMEM (Invitrogen) plus 10% fetal bovine serum (FBS) and penicillin-streptomycin-glutamine (PSG). BJ-5ta cells were cultured in four parts DMEM (Invitrogen) and one part Medium 199 (Invitrogen) supplemented with 10% FBS, PSG, and 0.01 mg/ml hygromycin B (Invitrogen).

### Constructs

CSII-pEF-H2B-mTurquoise and CSII-pEF-DHB(aa994-1087)-mVenus (Spencer et al., 2013) were described previously. cDNAs for Geminin (aa1-110) (Sakaue-Sawano et al., 2008) fused to mCherry, Cdt1 (aa30-120) fused to mVenus (Sakaue-Sawano et al., 2008), AuroraA fused to mCitrine, and Emi1 fused to mCitrine were cloned into the CSII-pEF lentiviral vector. Transduced cells were sorted on a Becton Dickinson Influx to obtain pure populations expressing the desired fluorescent reporters. Aurora A K162R mutation was made in the CSII-pEF-AuroraA-mCitrine construct using the Gibson assembly method with the mutation encoded in the primers. Mutant versions of mChy-APC-degron were constructed using synthesized gBlocks (Integrated DNA Technologies, IDT) and assembled into CSII-pEF-mCherry using the Gibson assembly method. Briefly, both KEN boxes (aa13-15 and aa87-89) were mutated to AAA to generate the APC-degron KEN mutant. The RxxL motif at aa 23-26 was further mutated to AxxA in the KEN mutant background to generate the APC-degron KEN/RxxL mutant.

### Image Processing

Mean nuclear intensities were measured by averaging the background-subtracted pixel intensities in each nucleus as defined by a nuclear mask. The nuclear mask was established by performing segmentation on H2B-mTurquoise images as follows. Log-transformed images were convolved with a rotationally symmetric Laplacian of Gaussian filter and objects were defined as contiguous pixels exceeding a threshold filter score. In order to segment cells in contact with their nearest neighbor, a custom segmentation algorithm was implemented to detect and bridge concave inflections in the perimeter of each object (hereafter referred to as the 'deflection bridging algorithm'). The deflection bridging algorithm was implemented on every identified object in the first imaging frame, and then only adaptively in subsequent frames. This was accomplished by iteratively tracking cells in each frame, detecting probable merge events (as discussed below), and selectively implementing the deflection bridging algorithm on putative merged objects. This method reduced the probability of over-segmentation, increased processing speed, and improved tracking fidelity.

Local background subtraction was performed on images of sensors or antibodies that were nuclear in subcellular distribution. For local background subtraction, the nuclear mask was expanded by 25μm and the background for each cell was calculated as the median pixel intensity of local non-masked pixels. For cytoplasmically localized sensors, the nuclear mask was dilated by 50μm, and the global background was calculated as the mode intensity of all non-masked pixels. As before, Cdk2 activity was calculated as the ratio of cytoplasmic to nuclear mean DHB fluorescence, with the cytoplasmic component calculated as the mean of the top 50$^{th}$ percentile of a ring of pixels outside of the nuclear mask.

Tracking of cells between frames was implemented by screening the nearest future neighbor for consistency in total H2B-mTurquoise fluorescence. This 'conservation of mass' was further exploited to detect merges or splits, which allowed recovery of overlapping traces. Finally, mitosis events (called at

anaphase) were called when the total H2B fluorescence of the two nearest future neighbors of a given cell were both between 45-55% of the total H2B fluorescence of the past cell.

**siRNA transfection**

MCF-10A cells were transfected using Dharmafect 1 (Thermo Scientific) according to the manufacturer's instructions. The following siRNAs were used: control siRNA (nontargeting #2, Dharmacon), siGenome pooled set of four siRNAs for cyclin A2, siGenome pooled set of four for Emi1, siGenome pooled set of four for Fzr1 (Cdh1), siGenome pooled set of four for Usp37, siGenome pooled set of eight for cyclin E1 and E2, siGenome pooled set of 12 for cyclin D1, D2, and D3 (Dharmacon) at final concentrations of 20nM unless noted. Six hours post-transfection, cells were washed with full growth medium and then imaging was immediately started. Cells were only considered if they went through one mitosis within the imaging period. This method works efficiently since all the genes targeted in this study are known to be degraded during or prior to the onset of mitosis. Thus, the siRNA would prevent subsequent accumulation in the next cell cycle.

**APC activity calculations**

The level of the APC-degron reporter in a cell is controlled by competing protein synthesis and degradation (Equation 1). The synthesis rate ($k_{synth}$) can be assumed to be constant due to the constitutive promoter of the APC-degron reporter (see Figures S1M and N). Based on our inhibitory experiments which suggest that the reporter degradation is mostly driven by APC, the degradation rate ($k_{deg}$) of the APC-degron reporter at a given time can be considered to be a product of a relative APC activity ($k_{APC}$) times the APC-degron concentration (Equation 2) (Xu and Qu, 2012). In this definition, relative APC activity reflects the relative concentration of substrate molecules converted per unit time, and has the units of 1/time.

We substituted $k_{deg}$ from Equation 2 into Equation 1 to obtain Equation 3. By rearranging the terms in Equation 3, the APC activity ($k_{APC}$) is equal to the rate of synthesis of APC-degron minus the change in APC-degron levels over time, divided by the APC-degron level (Equation 4). All of the terms in Equation 4 can be directly measured using the APC-degron reporter and live-cell time-lapse imaging, allowing one to calculate a relative APC activity ($k_{APC}$). Specifically, we measured $k_{synth}$, the change in APC-degron over time in single cells by measuring the slope of APC-degron increase after treatment with the proteasome inhibitor MG132 (10μM; see Figure S1I,J and M). We also used MG132 to ensure that the reporter during S and G2 is not measurably degraded by the proteasome, arguing that the rate of increase of the reporter can be used as a direct measure of the reporter synthesis rate in a particular cell. We then used the first derivative of the APC-degron levels as a measure of the change in APC-degron over time (dAPCdegron/dt) and used Equation 4 to calculate $k_{APC}$. Normalized to the maximum, this rate $k_{APC}$ can be considered to be a relative APC activity with the unit of 1/time. Implicit in this definition is an assumption that the rate of degradation of a ubiquitinated APC-degron by the proteasome is constant over the cell cycle and relatively fast compared to the conjugation of ubiquitins to the reporter by the APC. Thus, we are making the plausible assumption that APC-mediated ubiquitination is the rate-limiting step in APC-degron degradation (Xu and Qu, 2012). Furthermore, given the near identical time course for different endogenous APC substrates that we tested, this relative APC activity rate measured for the APC reporter likely reflects the kinetics of degradation also for other APC substrates.

**Equation 1)** $$\frac{\mathrm{dAPCdegron}}{\mathrm{dt}} = \mathrm{k_{synth}} + \mathrm{k}_{deg}$$

**Equation 2)** $$k_{deg} = -k_{APC}[\mathrm{APCdegron}\,]$$

**Equation 3)** $$\frac{\mathrm{dAPCdegron}}{\mathrm{dt}} = \mathrm{k_{synth}} - k_{APC}[\mathrm{APCdegron}\,]$$

**Equation 4)** $$k_{APC} = \frac{k_{synth} - \frac{dAPCdegron}{dt}}{[APCdegron]}$$

The percent suppression of APC activity at the G1/S transition can be calculated by comparing the levels of APC-degron at the two-steady states: $APC^{on}$ and $APC^{off}$ (see Equations 5-7). When the APC was off, we observed APC-degron accumulating at a constant rate for at least 24 hours. We did not track accumulation for periods longer than 24 hours due to length of the imaging session and also because cells that enter mitosis rapidly degrade the APC-degron. Thus we did not observe the maximum reached APC-degron levels at steady-state ($APC^{off}$). However, the average maximum levels we did observe was ~1000 relative fluorescent units with the real maximal level likely being a few fold higher (a.u.) (see Figure S2B). To measure the basal APC-degron levels ($APC^{on}$) we compared the fluorescent levels of APC-degron with non-expressing cells. We did not observe fluorescent signals above background which had a mean intensity of 12 a.u. during G1 (see Figure S2A). Therefore, we observed a greater than 100-fold change in APC-degron levels, arguing that $APC^{Cdh1}$ is inactivated greater than 99% when cells transition from G1 to S phase. Using estimated averaged steady state APC reporter levels of 2000 r.u. ($APC^{off}$) and residual averaged levels in G1 of maybe 2 r.u. when the background is considered ($APC^{on}$)., the inactivation of APC at the G1/S transition in a typical cell might be as high as 1000-fold.

**Equation 5)** $$\text{Steady-State}_{\text{APC on}} \quad 0 = k_{synth} - APC_{ON}(\text{Basal APCdegron level})$$

**Equation 6)** $$\text{Steady-State}_{\text{APC off}} \quad 0 = k_{synth} - APC_{OFF}(\text{Max APCdegron level})$$

**Equation 7)** $$\text{APC Suppression Ratio} = \frac{APC_{OFF}}{APC_{ON}} = \frac{\text{Basal APCdegron level}}{\text{Max APCdegron level}}$$

In experiments using cycling cells, the relative APC activity was normalized to the maximum APC activity measured during the imaging period for each cell. Only cells that were observed to have gone through mitosis were considered for analysis since APC-degron reporter levels during G1 phase are indistinguishable from background which makes it difficult to measure a maximal APC activity during G1 phase. The rapid onset of the degradation of the APC-degron reporter during mitosis, when APC-degron levels go from very high to very low, allows one to directly measure a lower limit for the relative APC activity change in each cell. This drop in APC reporter level at mitosis is in each cell greater than 99%, again arguing that the activity of APC in S and G2 is greatly suppressed. In some experiments, addition of MG132 and single-cell measurements of $k_{synth}$ was not feasible. In these cases, we used a single APC-degron synthesis rate for all cells. We calculated the population-level synthesis rate by measuring the slope of APC-degron increase during S and G2 phase for thousands of cells and used the median slope (Figure S1L and M).

**RNA FISH and quantification of mRNA amount per cell**

RNA *in situ* hybridization was carried out using the Affymetrix Quantigene ViewRNA ISH cell assay. A probe was custom designed to target Emi1 or E2F1. Cells in a 96-well glass plate (Greiner) were fixed with 4% paraformaldehyde for 15 min and dehydrated overnight using 75% EtOH. After rehydration in PBS for 10 min, the cells were permeabilized with a detergent solution for 5 min and then treated with Proteinase K for 15 min at room temperature. The probes were then diluted 1:25 with hybridization buffer and incubated at 40°C for 3 hrs. Cells were then hybridized with the three different probes in succession: preamplification probe, amplification probe, and label probe. Cells were washed three times with washing buffer between each hybridization step, and all hybridizations were performed by incubating cells with a probe for 30 min at 40°C. Finally, cells were incubated with Hoechst (1:10,000 in PBS) for 5 min, washed three times with PBS, and left in PBS for imaging. Image analysis was carried out using a custom-written MATLAB script. Briefly, images were subjected to background subtraction followed by a log (Laplacian of Gaussian) filter designed to identify single foci. The images were subsequently passed through a predetermined threshold to identify all foci originating from RNA molecules. Next, each focus was associated with the closest nucleus (as identified by Hoechst staining) to measure the total mRNA

levels of individual cells. RNA molecules that were too far away from any cell less than ~60 μm) were disqualified from further analysis. Finally, we quantified the total amount of mRNA by summing the intensities of all identified puncta to account for foci that were created from two (or more) proximate molecules.